

Prevention of Proliferative Vitreoretinopathy by Suppression of Phosphatidylinositol 5-Phosphate 4-Kinases

Gaoen Ma,¹⁻⁴ Yajian Duan,¹⁻³ Xionggao Huang,¹⁻³ Cynthia X. Qian,^{2,3} Yewlin Chee,^{2,3} Shizuo Mukai,^{2,3} Jing Cui,⁵ Arif Samad,⁶ Joanne Aiko Matsubara,⁵ Andrius Kazlauskas,¹⁻³ Patricia A. D'Amore,¹⁻³ Shuyan Gu,⁴ and Hetian Lei¹⁻³

¹Schepens Eye Research Institute, Boston, Massachusetts, United States

²Massachusetts Eye and Ear, Boston, Massachusetts, United States

³Department of Ophthalmology, Harvard Medical School, Boston, Massachusetts, United States

⁴Aier School of Ophthalmology, Central South University, Changsha, Hunan Province, China

⁵The University of British Columbia, Vancouver, British Columbia, Canada

⁶Dalhousie University, Halifax, Nova Scotia, Canada

Correspondence: Hetian Lei, Schepens Eye Research Institute, Massachusetts Eye and Ear, Department of Ophthalmology, Harvard Medical School, 20 Staniford Street, Boston, MA 02114, USA; hetian_lei@meei.harvard.edu.

GM and YD contributed equally to the work presented here and should therefore be regarded as equivalent authors.

Submitted: February 23, 2016

Accepted: June 9, 2016

Citation: Ma G, Duan Y, Huang X, et al. Prevention of proliferative vitreoretinopathy by suppression of phosphatidylinositol 5-phosphate 4-kinases. *Invest Ophthalmol Vis Sci*. 2016;57:3935-3943. DOI:10.1167/iov.16-19405

PURPOSE. Previous studies have shown that vitreous stimulates degradation of the tumor suppressor protein p53 and that knockdown of phosphatidylinositol 5-phosphate 4-kinases (PI5P4K α and β) abrogates proliferation of p53-deficient cells. The purpose of this study was to determine whether vitreous stimulated expression of PI5P4K α and β and whether suppression of PI5P4K α and β would inhibit vitreous-induced cellular responses and experimental proliferative vitreoretinopathy (PVR).

METHODS. PI5P4K α and β encoded by *PIP4K2A* and *2B*, respectively, in human ARPE-19 cells were knocked down by stably expressing short hairpin (sh)RNA directed at human *PIP4K2A* and *-2B*. In addition, we rescued expression of PI5P4K α and β by re-expressing mouse *PIP4K2A* and *-2B* in the PI5P4K α and β knocked-down ARPE-19 cells. Expression of PI5P4K α and β was determined by Western blot and immunofluorescence. The following cellular responses were monitored: cell proliferation, survival, migration, and contraction. Moreover, the cell potential of inducing PVR was examined in a rabbit model of PVR effected by intravitreal cell injection.

RESULTS. We found that vitreous enhanced expression of PI5P4K α and β in RPE cells and that knocking down PI5P4K α and β abrogated vitreous-stimulated cell proliferation, survival, migration, and contraction. Re-expression of mouse PIP4K α and β in the human PI5P4K α and β knocked-down cells recovered the loss of vitreous-induced cell contraction. Importantly, suppression of PI5P4K α and β abrogated the pathogenesis of PVR induced by intravitreal cell injection in rabbits. Moreover, we revealed that expression of PI5P4K α and β was abundant in epiretinal membranes from PVR grade C patients.

CONCLUSIONS. The findings from this study indicate that PI5P4K α and β could be novel therapeutic targets for the treatment of PVR.

Keywords: proliferative vitreoretinopathy, PI5P4Ks, vitreous

Proliferative vitreoretinopathy (PVR) develops in 8% to 10% of patients who undergo reparative primary retinal detachment surgery¹⁻⁷ and in 40% to 60% of patients with open globe injury.^{1,8-16} The major feature of PVR is the formation of a subretinal or epiretinal membrane (ERM) that consists of retinal pigment epithelial (RPE) cells, fibroblasts, glial cells, and macrophages, as well as extracellular matrix.²⁻⁷ The ERM may be attached to the retina and subsequently contract, causing a new retinal detachment or failure of a surgically corrected detachment.²⁻⁷ At present, repeat surgery is the only option for treating PVR; however, the surgery has had poor functional results.

We have recently shown that vitreous from rabbits and patients with PVR preferentially activates the signaling pathway of PDGF receptor (PDGFR) α /phosphoinositide 3 kinase (PI3K)/

Akt,¹⁷ leading to the phosphorylation of murine double minute 2 (MDM2), an oncogene protein acting as an E3 ubiquitin ligase.¹⁸⁻²⁰ Phosphorylation of MDM2 increases its interaction with the tumor suppressor protein p53, promoting p53 degradation.²¹ The activation of p53 can lead to cell cycle arrest, apoptosis, and/or senescence.²²

The codon 72 polymorphisms (rs1042522) in human p53 protein contain two variants, Arg and Pro. The Arg 72 variant is associated with more apoptosis than is the Pro 72 variant.²³ The Arg 72 variant also interacts more readily with MDM2,^{24,25} which facilitates the export of p53 from the nucleus and its degradation through the ubiquitination pathway. Intriguingly, the Pro variant of p53 codon 72 polymorphisms is associated with a higher risk of developing PVR after a primary retinal detachment.²⁵ Nutin-3, a small molecule that blocks the

interaction of MDM2 with p53, prevents retinal detachment in experimental PVR in rabbits induced by intravitreal cell injection, but the cellular membranes still form in the vitreous.²¹ In addition, vitreous-induced cell contraction is stronger than that of cells with p53 suppressed by short hairpin (sh) RNA and without rabbit vitreous (RV) induction.²¹ Thus, it appears that other factors coordinate with p53 loss to promote vitreous-stimulated gel contraction as well as membrane formation in experimental PVR. Knowing that suppression of phosphatidylinositol 5-phosphate 4-kinases (PI5P4Ks) inhibits p53-null tumor growth,²⁶ we hypothesized that PI5P4Ks might participate in vitreous-induced cellular responses as well as in the pathogenesis of PVR.

Phosphatidylinositols (PIs), a family of phosphatidylglycerides, are synthesized by the phosphorylation at positions 3, 4, and 5 on the inositol ring. PI-4,5-bisphosphate (PI-4,5-P₂) is the major substrate for class I PI3Ks and plays a key role in mediating the localization of proteins to the plasma membrane.²⁷ The type II PI-5-P-4 kinases can catalyze the phosphorylation of PI-5-P at the 4-position to become PI-4,5-P₂. In humans and mice, there are three distinct type II kinases, PI5P4K α , - β , and - γ , encoded by PIP4K2A, -B and -C, respectively. The type I PIP kinases generate PI-4,5-P₂ at the plasma membrane, whereas the type II kinases are located at internal membranes, including the endoplasmic reticulum, Golgi, and nucleus, where they likely generate PI-4,5-P₂.^{26,28,29} The localized type II PI5P4Ks may be involved in the coordination with p53 loss.²⁶ Thus, suppression of PI5P4Ks is a candidate for inhibiting p53-loss-mediated cellular responses and pathology such as PVR.

In this study, we investigated the role of PI5P4Ks in the development of PVR, and found that knocking down both PI5P4K α and - β in human RPE (ARPE-19) cells inhibited vitreous-induced cell proliferation, survival, migration, and contraction as well as the development of experimental PVR in rabbits. In addition, Both PI5P4K α and - β were abundant in the ERMs of grade C PVR patients.

MATERIALS AND METHODS

Major Reagents and Cell Culture

Primary antibodies against p53, PI5P4K α , and PI5P4K β were purchased from Cell Signaling Technology (Danvers, MA, USA) and β -actin from Santa Cruz Biotechnology (Santa Cruz, CA, USA). Secondary antibodies, HRP (horseradish peroxidase)-conjugated goat anti-rabbit IgG and goat anti-mouse IgG, were purchased from Santa Cruz Biotechnology. Enhanced chemiluminescent substrate for detection of HRP was obtained from Pierce Protein Research Products (Rockford, IL, USA). Puromycin and carbenicillin were purchased from Sigma-Aldrich Corp. (St. Louis, MO, USA).

ARPE-19 (a spontaneously arising RPE cell line) cells were purchased from American Type Culture Collection (ATCC; Manassas, VA, USA), and RPEM cells were RPE cells originated from an ERM of a PVR patient as described previously.³⁰ Both ARPE-19 and RPEM cells were cultured in Dulbecco's modified Eagle's medium/nutrient mixture (DMEM/F12; Invitrogen, Grand Island, NY, USA) supplemented with 10% fetal bovine serum (FBS). Human embryonic kidney (HEK) 293T cells and primary rabbit conjunctival fibroblasts (RCFs)³¹ were cultured in DMEM with 10% FBS.

HEK 293GPG cells were HEK 293 cells expressing the foreign GAG and POL genes as well as the vesicular stomatitis virus (VSV)-G protein (pseudotyping retroviral envelope) of VSV. The VSV-G protein was kept not added during cell growth via a tetracycline-controlled transcriptional (TET) repressor in

these cells, which were grown in DMEM (4.5 g/L glucose) supplemented with 10% FBS, 1 μ g/mL tetracycline, 2 μ g/mL puromycin, 0.3 mg/mL G418, and 16.7 mM HEPES (Invitrogen). When producing virus, the culture medium used for HEK 293GPG was DMEM plus 10% FBS and 16.7 mM HEPES.

Knockdown of PI5P4K α and - β by shRNA

Escherichia coli strains containing plasmids *pLKO.1*-shRNA for *PIP4K2A* (TRCN000006009 and TRCN000006011) and *PIP4K2B* (TRCN000006013 and TRCN000006016) were purchased from Dharmacon (Lafayette, CO, USA), and an *E. coli* strain containing *pLKO.1-sbRNA* for green fluorescent protein (GFP) was obtained from Dana-Farber Cancer Institute (Boston, MA, USA). The respective *pLKO.1-sbRNA* lentiviral vector (1000 ng), the packaging plasmid *psPAX2* (12260; Addgene, Cambridge, MA, USA) (900 ng), and the envelope plasmid *VSV-G* (Addgene 8454) (100 ng) were mixed together and then added to a mixture of TranIT-LT1 (MIR 2300; Mirus Bio LLC, Madison, WI, USA) or lipofectamine 2000 (Invitrogen) 6 μ L with OPTI-MEM (Invitrogen 31985-070) 90 μ L. This transfection mix was incubated at room temperature for 30 minutes and then carefully transferred into a 60-mm cell culture dish with HEK 293T cells that were approximately 70% confluent without antibiotics. After 18 hours (37°C, 5% CO₂), the medium was replaced with growth medium supplemented with 30% FBS, and lentiviruses were harvested at 40 hours after the transfection. The viral harvest was repeated at 24-hour intervals three times. The virus-containing media were pooled and then centrifuged at 800g for 5 minutes, and the supernatant was used to infect cells of ARPE-19, RPEM, and RCFs supplemented with 8 μ g/mL polybrene. The infected cells were selected in media with puromycin (ARPE-19, RPEM: 4 μ g/mL; RCF: 2 μ L/mL), and the resulting cells were examined by Western blot.³²⁻³⁴

Expression of Mouse *PIP4K2A* and -*2B* in ARPE-19 Cells Whose PI5P4K α and - β Were Knocked Down by shRNA

The full-length cDNA of mouse *PIP4K2A* or *PIP4K2B* was subcloned from *pCMVSPORT6-PIP4K2A* (3672732; Thermo Scientific, Waltham, MA, USA) or *pCMVSPORT6-PIP4K2B* (6491155; Thermo Scientific) into a retroviral vector of *pLNCX3* (*LTR-CMV-Sall-HpaI-SacI-NotI-BglII-Clal-LTR*) derived from *pLNCX* (GenBank: M28247) (GenBank, National Institutes of Health, Bethesda, MD, USA) by *Sal I/Not I*, respectively. All the DNA sequences were confirmed by DNA sequencing at Massachusetts DNA Core Facility (Cambridge, MA, USA).

On the day of transfection, plasmid DNA (25 μ g) or a transfection reagent (Invitrogen: lipofectamine 2000, 156 μ L) was mixed individually with 1.8 mL OptiMEM (Thermo Scientific). The two were then mixed together and allowed to sit at room temperature for 45 minutes. The DNA mixture was added dropwise into approximately 70% confluent HEK 293GPG cells³⁴ with 10 mL OptiMEM in a 25-cm-diameter dish. After incubation for 7 to 10 hours, 12 mL virus-producing medium was added, and this day was considered day 0. At 24 hours post transfection, the media were replaced with the completed virus-producing medium. On days 2, 3, 4, and 5, the media were collected into 50-mL sterile conical tubes and spun at 800g for 5 minutes. The pooled supernatants were then pelleted in sterile tubes at 25,000g for 90 minutes to concentrate the viruses. Finally, the viral pellets were resuspended in 300 μ L sterile TNE buffer (50 mM Tris pH 7.8, 130 mM NaCl, 1 mM ethylenediaminetetraacetic acid [EDTA]), transferred into microtubes, and dissolved at 4°C with gentle

rotation overnight. These dissolved retroviruses were then used to infect target cells with 8 µg/mL polybrene or kept at -80°C .³²⁻³⁴ Expression of *pLNCX3-PIP4K2A* and *-2B* in the ARPE-19 cells was selected in the 2 mg/mL G418-contained culture medium for 2 weeks and then analyzed by Western blot.

Western Blot

Cells grown to 90% confluence in wells of 24-well plates were serum starved for 24 hours, and then treated with or without normal RV (diluted 1:2 in DMEM/F12) for 16 hours. After two washes with ice-cold phosphate-buffered saline (PBS), the cells were lysed in 1× sample buffer diluted with protein extraction buffer [10 mM Tris-HCl, pH 7.4; 5 mM EDTA, 50 mM NaCl, 50 mM NaF, 1% Triton X-100, 20 µg/mL aprotinin, 2 mM Na_3VO_4 , 1 mM phenylmethylsulfonyl fluoride] from 5× sample buffer [25 mM EDTA, 10% sodium dodecyl sulfate (SDS), 500 mM dithiothreitol (DTT), 50% sucrose, 500 mM Tris-HCl (pH = 6.8), 0.5% bromophenol blue]. The samples were boiled for 5 minutes and then centrifuged for 5 minutes at 13,000g, 4°C . Proteins in the samples were separated by 10% SDS-polyacrylamide gel electrophoresis (PAGE), transferred to polyvinylidene difluoride (PVDF) membranes, and then subjected to Western blot analysis using selected antibodies. Signal intensity was determined by densitometry using NIH ImageJ software.³²⁻³⁴

Cell Proliferation Assay

ARPE-19 cells with shRNA for *GFP* or *PIP4K2A/2B* were seeded into wells of a 24-well plate at a density of 3×10^4 cells/well in DMEM/F12 with 10% FBS. Following attachment, the cells were treated with DMEM/F12 or RV (1:2 dilution in DMEM/F12). On day 3, the cells were trypsin detached from the plates and counted in a hemocytometer. Each experimental condition was assayed in duplicate, and at least three independent experiments were performed.^{32,33}

Cell Apoptosis Assay

ARPE-19 cells with shRNA for *GFP* or *PIP4K2A/2B* were seeded into 6-cm dishes at a density of 2×10^5 cells per dish in DMEM/F12 + 10% FBS. Following attachment, the cells were treated with DMEM/F12 or RV (1:2 dilution in DMEM/F12). On day 3, the cells were stained with fluorescein isothiocyanate (FITC)-conjugated annexin V and propidium iodide (PI) following the manufacturer's instructions (BD Biosciences, Palo Alto, CA, USA). The cells were analyzed by flow cytometry in a Beckman Coulter XL instrument (Brea, CA, USA). At least three independent experiments were performed.^{32,33}

Cell Migration Assay

ARPE-19 cells with shRNA for *GFP* or *PIP4K2A/2B* in a 12-well plate were grown to near confluence, and then a wound was created by scratching the monolayer with a 200-µL pipette tip.³⁴ The cells were washed with PBS and treated with DMEM/F12 or RV (1:2 dilution in DMEM/F12). The scratched area was photographed to capture the initial width and photographed again 16 hours later. Analysis was conducted using Adobe Photoshop CS4 software (San Jose, CA, USA). At least three independent experiments were performed.

Collagen Contraction Assay

Cells were resuspended in 1.5 mg/mL neutralized collagen I (INAMED, Fremont, CA, USA) (pH 7.2) on ice at a density either of 1×10^6 for RPE cells/mL or of 1×10^5 for RCF cells/mL.^{31,33}

The mixture was transferred into wells of 24-well plates that had been preincubated overnight with 5 mg/mL BSA/PBS. After the collagen had polymerized at 37°C for 90 minutes, 0.5 mL DMEM/F12 or RV (1:2 dilution in DMEM/F12) was added. On day 3, the gel diameter was measured and the gel area calculated using the formula $3.14 \times r^2$, where r is the radius of the gel. At least three independent experiments were performed.^{33,35}

Experimental PVR in Rabbits

As previously described,^{35,36} PVR was induced in the right eyes of Dutch Belted rabbits purchased from Covance (Denver, PA, USA). Briefly, a gas vitrectomy was performed by injecting 0.1 mL perfluoropropane (C_3F_8) (Alcon, Fort Worth, TX, USA) into the vitreous cavity 4 mm posterior to the corneal limbus. One week later, all rabbits were injected with 0.1 mL platelet-rich plasma (PRP) from rabbits and 0.1 mL DMEM/F12 containing either 3.0×10^5 cells of ARPE-19 (10 rabbits) or 1.0×10^5 of RCFs (5 rabbits) with shRNA for *GFP* or *PIP4K2A/2B* under a surgical microscope. The retinal status was examined with an indirect ophthalmoscope through a +30 D fundus lens on days 1, 3, 5, 7, 14, 21, and 28 by two double-masked ophthalmologists. Proliferative vitreoretinopathy was graded according to the Fastenberg classification from 0 through 5.³⁷ On day 28, animals were killed, the eyes were enucleated, and the eyeballs were either fixed with 10% formalin for histology analysis or frozen at -80°C for vitreous extraction. All surgeries were performed under aseptic conditions and adhered to the ARVO Statement for the Use of Animals in Ophthalmic and Vision Research. The protocol for the use of animals was approved by the Schepens Animal Care and Use Committee (Boston, Massachusetts).

Rabbit vitreous was prepared from frozen rabbit eyeballs as described previously.³⁴ The left eyes were not manipulated in any way and were normal and free of obvious abnormalities.

Optical Coherence Tomography (OCT)

Fundus photographs and OCT were taken using a spectral domain (SD)-OCT system (Bioptigen, Inc., Durham, NC, USA). Rabbits were deeply anesthetized with intramuscular anesthesia consisting of ketamine 30 to 50 mg/kg body weight, xylazine 5 to 10 mg/kg body weight, and acepromazine 1 mg/kg body weight. Depth of anesthesia was verified by the absence of the toe pinch withdrawal reflex. The pupils were dilated with topical 1% tropicamide to view the fundus.^{38,39}

Immunofluorescence

Frozen sections of embedded frozen ERMs from three patients with grade C PVR were prepared as described previously,⁷ and this research adhered to the Tenets of the Declaration of Helsinki and the protocol approved by the Schepens Eye Research Institute Massachusetts Eye and Ear Institutional Review Board (632172-3). The sections were fixed in 3.7% formaldehyde/PBS for 10 minutes and were then treated for 15 minutes with 0.3% hydrogen peroxide (to remove endogenous peroxidases). Subsequently, the sections were preincubated with 5% normal goat serum in 0.3% Triton X-100/PBS for 20 minutes, then incubated with primary antibodies against PI5P4K α or PI5P4K β (1:100 dilution) for 1 hour or with a normal rabbit IgG. After three washes with PBS, the sections were incubated with fluorescently labeled secondary antibodies, Dylight 549 (Vector Laboratories, Inc., Burlingame, CA, USA) (1:300 dilution in a blocking buffer), for 30 minutes. After three washes with PBS, the slides were mounted with a mounting medium containing 4',6'-diamidino-2-phenylindole

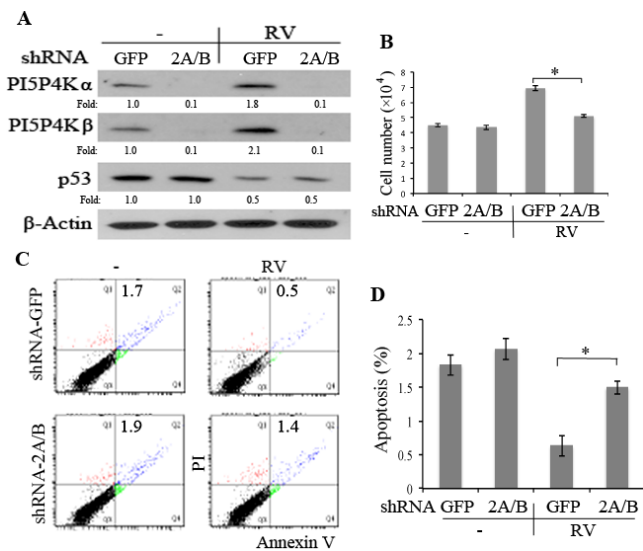


FIGURE 1. Knockdown of PI5P4K α and β in ARPE-19 cells led to the suppression of vitreous-stimulated proliferation and survival. (A) ARPE-19 cells expressing shRNA for *GFP* (GFP) or *PIP4K2A/B* (2A/B) were treated for 16 hours with or without rabbit vitreous (RV) diluted (1:2) in DMEM/F12. The cell lysates were subjected to Western blot analysis using the indicated antibodies. Fold change was calculated by first normalizing PI5P4K α and β for β -actin and then calculating the ratio of the basal (shGFP) to stimulated protein levels for each cell type. This is representative of three independent experiments. (B) The characterized ARPE-19 cells in (A) were seeded into wells of a 24-well plate at a density of 3×10^4 cells/well in DMEM/F12 plus 10% FBS. Following cell attachment, the medium was replaced with 0.5 mL DMEM/F12 or RV diluted (1:2) in DMEM/F12. The cells were counted with a hemocytometer on day 3. The mean \pm standard deviation (SD) of three independent experiments is shown; * $P < 0.05$ using an unpaired *t*-test. (C) The characterized ARPE-19 cells in (A) were seeded into 6-cm dishes in DMEM/F12 + 10% FBS at a density of 2×10^5 cells per dish. After 8 hours, the cells were treated with or without RV. On day 3, the cells were analyzed for apoptosis by FACS (fluorescence-activated cell sorting). An example of the raw FACS data is shown. PI, propidium iodide; FITC, fluorescein isothiocyanate conjugated with annexin V for determining apoptosis. (D) The mean \pm SD of three independent experiments described in (C) is shown; * $P < 0.05$ using an unpaired *t*-test.

(DAPI) (Vector Laboratories) and photographed under a fluorescence microscope.^{21,40}

PVR Patient Vitreous

As previously described,³³ human vitreous (HV) samples from PVR patients (1.0–1.5 mL) were obtained during pars plana vitrectomy performed before initiating the pars plana infusion at the Vancouver Hospital, British Columbia. Ethics approval was obtained before the initiation of this project from the Vancouver Hospital and University of British Columbia Clinical Research Ethics Board. The University of British Columbia Clinical Research Ethics Board policies comply with Tri Council Policy and Good Clinical Practice Guidelines, which have their origins in the ethical principles in the Declaration of Helsinki. Written informed consent was obtained from patients.

Statistics

The data were analyzed using an unpaired *t*-test or a Mann-Whitney test. A power (*p*) value less than 0.05 was considered statistically significant.

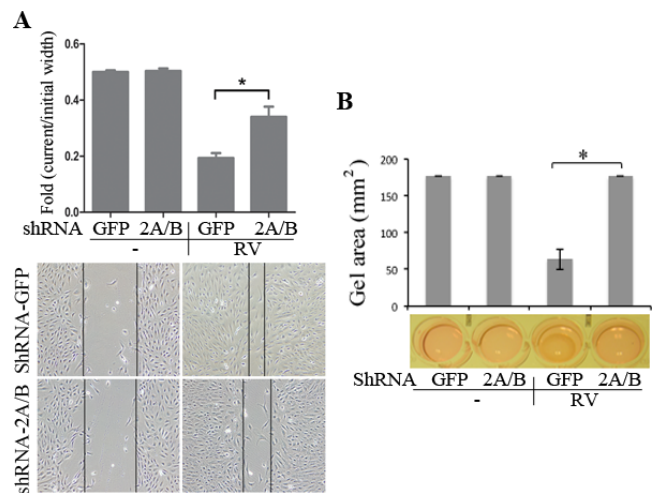


FIGURE 2. Suppression of PI5P4 α and β blunted RV-stimulated migration and contraction of ARPE-19 cells. (A) ARPE-19 cells expressing shRNA for *GFP* (GFP) or *PIP4K2A/B* (2A/B) were cultured to near confluence in wells of 12-well plates, and the cell monolayer was scratched using a 200- μ L pipette tip and photographed to document the initial wound width. The cells were then washed and treated with or without RV. Sixteen hours later, images of cells were taken again and analyzed for the wound width using Adobe Photoshop CS4 software. The mean \pm SD of three independent experiments is shown (*top*). * $P < 0.05$ using an unpaired *t*-test. Representative of raw data of three independent experiments (*bottom*) is shown. Scale bar: 500 μ m. (B) The ARPE-19 cells expressing shRNA for *GFP* (GFP) or *PIP4K2A/B* (2A/B) were resuspended in 1.5 mg/mL neutralized collagen (pH 7.2) at a density of 1×10^6 cells/mL and seeded into wells of a 24-well plate that had been preincubated overnight with 5 mg/mL BSA/PBS. The collagen was polymerized at 37°C for 90 minutes. The collagen gels were overlaid with DMEM/F12 alone (-) or RV. On day 3, the gel diameter was measured and calculated using the formula $[3.14 \times (\text{diameter}/2)^2]$. The mean \pm SD of the three independent experiments is shown; * $P < 0.05$ using an unpaired *t*-test. A photograph of a representative experiment is shown at the *bottom of the bar graphs*.

RESULTS

Suppression of PI5P4Ks in ARPE-19 Cells Attenuates Vitreous-Induced Cell Proliferation and Survival

Vitreous induces degradation of p53,^{17,21} whose loss coordinates elevation of PI5P4K α and β to improve proliferation and survival of cancer cells.²⁶ Thus, we speculated that vitreous might enhance expression of PI5P4K α and β . As predicted, the treatment of ARPE-19 cells with RV for 16 hours increased expression of PI5P4K α and β (Fig. 1A). It has been shown that knockdown of both PI5P4K α and β in p53-deficient cancer cells abrogates cell proliferation.²⁶ Therefore, we reasoned that suppression of PI5P4K α and β might inhibit RV-induced cell proliferation and survival. To investigate this possibility, we knocked down PI5P4K α and β effectively by two independent shRNAs targeting these proteins in ARPE-19 cells (Fig. 1A), and then treated these cells with or without RV. On day 3, the cell number was determined. As shown in Figure 1B, RV stimulated cell proliferation, which is consistent with previous findings.³⁵ Interestingly, knockdown of PI5P4K α and β did not affect the basal proliferation of ARPE-19 cells but did block RV-stimulated cell proliferation (Fig. 1B). Furthermore, suppression of PI5P4K α and β by shRNA did not impact serum starvation-induced apoptosis of ARPE-19 cells, but did abrogate RV-mediated protection from apoptosis (Figs. 1C, 1D). These

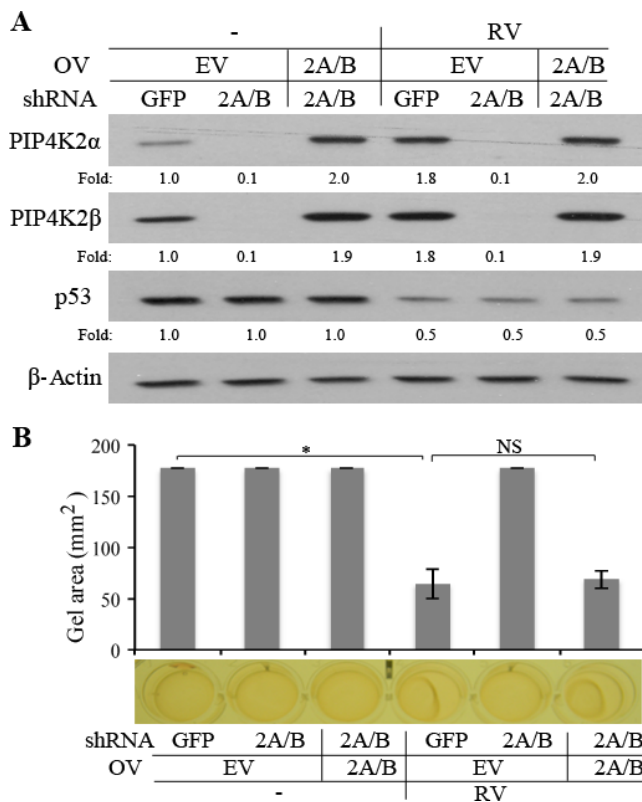


FIGURE 3. Expression of mouse *PIP4K2A/B* restored RV-induced contraction of ARPE-19 cells whose endogenous *PI5P4α* and β were suppressed by shRNAs. (A) Mouse *PIP4K2A* and *PIP4K2B* (2A/B) were overexpressed (OV) in ARPE-19 cells whose endogenous *PI5P4α* and β were suppressed by shRNAs through introduction of *pLNCX3-PIP4K2A-PIP4K2A/B* into these cells. The cells with an empty retroviral vector (EV) *pLNCX3* served as controls. These cells were then treated for 16 hours with or without RV, and their lysates were subjected to Western blot analysis using the antibodies indicated as described in Figure 1A. This is representative of three independent experiments. (B) The characterized ARPE-19 cells in (A) were assessed for their ability to contract as described in the legend of Figure 2B. The mean \pm SD of the three independent experiments is shown; * $P < 0.05$ using an unpaired *t*-test, and NS indicates no significant difference between the groups. A photograph of a representative experiment is shown at the bottom of the bar graphs.

results demonstrate that suppression of *PI5P4Kα* and β attenuates RV-induced cell proliferation and survival against apoptosis, processes intrinsic to the pathogenesis of PVR.³⁵

Knockdown of *PI5P4Ks* in ARPE-19 Cells Blocks Vitreous-Stimulated Cell Migration and Contraction

PI5P4Kα and β can convert PI-5-P to PI-4,5-P₂, which regulates actin filament elongation and interaction of the plasma membrane with the cytoskeleton.⁴¹⁻⁴³ Next, we asked whether knockdown of *PI5P4Kα* and β impacted RV-induced cell migration and contraction. As shown in Figure 2, suppression of *PI5P4Kα* and β did not affect cell migration and contraction in the serum-starved cells, but did blunt RV-induced migration and contraction of ARPE-19 cells. These experiments demonstrate that suppression of *PI5P4Kα* and β blunts RV-induced increase in cellular responses intrinsic to the pathogenesis of PVR, suggesting that knockdown of *PI5P4Kα* and β might be able to inhibit the development of PVR.

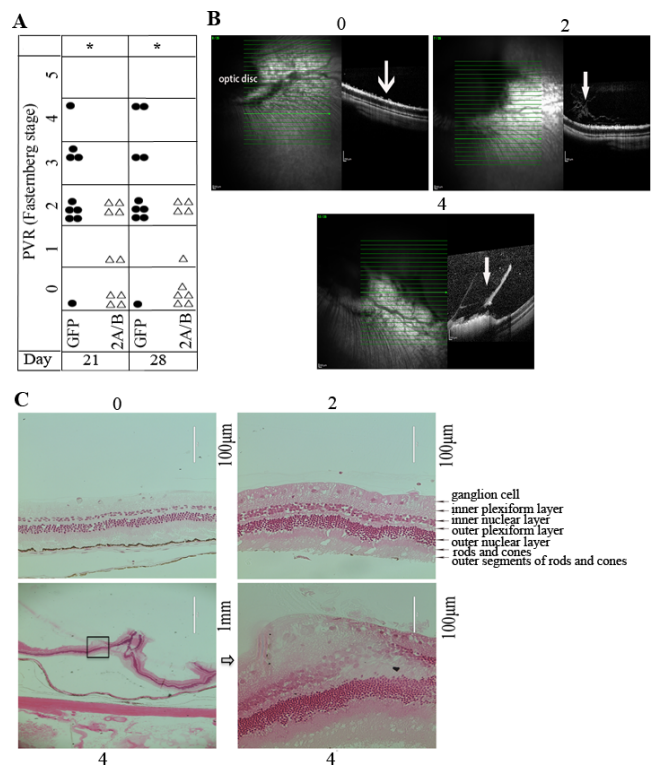


FIGURE 4. Suppression of *PI5P4Kα* and β in ARPE-19 cells prevented experimental PVR. (A) PVR was induced in the right eyes of Dutch Belted rabbits as previously described.^{33,36} Briefly, 1 week after gas vitrectomy, rabbits were intravitreally injected with 0.1 mL PRP and ARPE-19 cells (3×10^5) expressing shRNA for *GFP* (GFP) or *PIP4K2A/B* in 0.1 mL DMEM/F12 (2A/B). The rabbits were examined on days 1, 3, 5, 7, 14, 21, and 28 with an indirect ophthalmoscope. The PVR status for each rabbit was plotted on days 21 and 28. The data were subjected to Mann-Whitney analysis. *A significant difference between the two groups (GFP and $-2A/B$). (B) Rabbits with PVR representative of stages 0, 2, and 4 were imaged by OCT. Arrows in 0, 2, and 4 point to a normal, a fibrotic, and a pathologic retina with fibrosis banding, respectively. The numbers 0, 2, and 4 at the top of each indicate retinal images from rabbits with PVR stages 0, 2, and 4, respectively. (C) Eyeballs from rabbits with PVR stages 0, 2, and 4 were fixed, sectioned, and stained with hematoxylin and eosin. The retina section with PVR stage 4, has been enlarged to in the bottom right to show that there was growth of fibrosis in the abnormal, thicker retina.

Expression of Mouse *PIP4K2A/2B* Restores the Ability of RV-Induced Proliferation and Contraction of *PI5P4Kα*- and β -Deficient ARPE-19 Cells

To exclude unknown nonspecific targets of shRNAs for human *PIP4K2A/2B*, we expressed mouse *PIP4K2A/2B* in ARPE-19 cells whose endogenous *PI5P4Kα* and β had been knocked down by shRNAs. As shown in Figure 3A, expression of mouse *PI5P4Kα* and β was comparable to RV-induced expression of *PI5P4Kα* and β in ARPE-19 cells. Importantly, expressing mouse *PI5P4Kα* and β restored the capability of RV-induced contraction (Fig. 3B) of the *PI5P4Kα*- and β -deficient cells. These experiments indicate that RV-induced expression of *PI5P4Kα* and β coordinates with p53 loss to promote cell contraction and that *PI5P4Kα* and β constitute a potential therapeutic target for treatment of PVR.

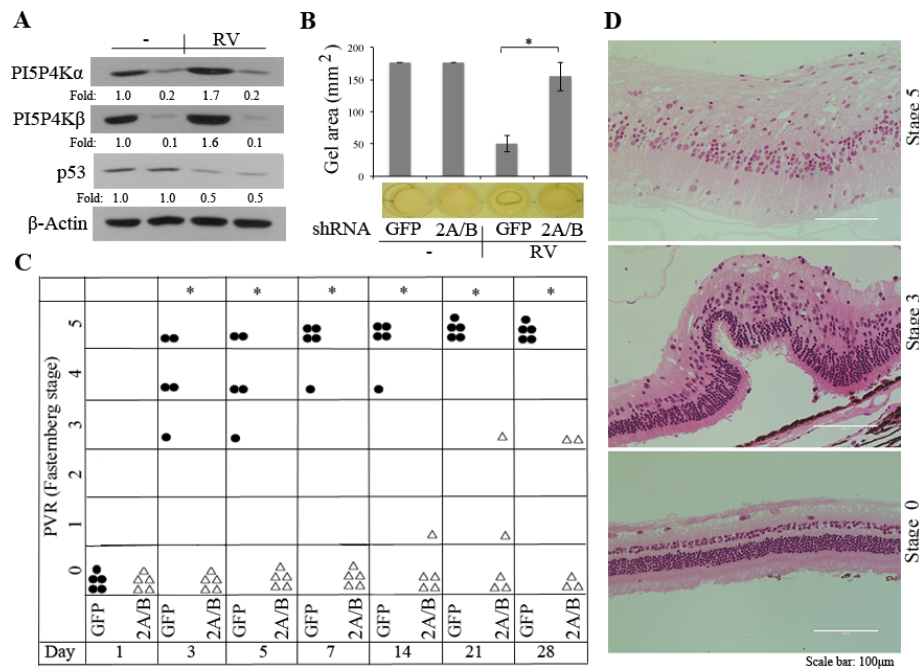


FIGURE 5. Knockdown of PI5P4K α and β in RCF cells abrogated their ability to induce PVR. (A) RCF cells expressing shRNA for GFP (GFP, as a control) or PIP4K2A/B (2A/B) were treated with or without RV for 16 hours. The cell lysates were subjected to Western blot analysis using the antibodies indicated. The data are representative of three independent experiments. (B) The characterized RCF cells in (A) were examined for their ability to contract as described in the legend of Figure 2B. The mean \pm SD of the three independent experiments is shown; * $P < 0.05$ using an unpaired t -test. A photograph of a representative experiment is shown at the bottom of the bar graphs. (C) PVR was induced in the right eyes of Dutch Belted rabbits by intravitreal injection of RCF (1×10^5) as in Figure 4. The data were subjected to Mann-Whitney analysis. *A significant difference between the two groups. (D) Representative eyeballs from rabbits with PVR stages 0, 3, and 5 were fixed, sectioned, and stained with hematoxylin and eosin. In the eyes with PVR stage 5, the retina was thicker than that in PVR stage 0.

Suppression of PI5P4K α and β in ARPE-19 Cells Prevents Experimental Retinal Detachment

During PVR pathogenesis, a major characteristic is the formation of an ERM that consists of cells including RPE cells and fibroblasts as well as extracellular matrix.^{9,36} To examine the effect of PI5P4K α and β knockdown on the development of PVR, we injected rabbit eyes intravitreally with ARPE-19 cells in which PI5P4K α and β were suppressed by shRNA.³⁵ Cells with shGFP were used as controls. As shown in Figure 4A, while there was some fibrosis in 50% of the rabbits, none of the rabbits injected with ARPE-19 cells with shPI5P4K α and β progressed to retinal detachment (Figs. 4A, 4B). However, retinal detachment developed in 40% of rabbits injected with ARPE-19 with shGFP control cells (Figs. 4A, 4B). Histologic analysis indicated fibrotic growth from the retina in stage 4 PVR induced by shGFP ARPE-19 cells in rabbits (Fig. 4C), whereas none of the rabbits injected with shPI5P4K α and β ARPE-19 cells displayed this pathologic characteristic.

Suppression of PI5P4K α and β in RCF Cells Abrogates Experimental PVR

Our previous observations demonstrated that RCFs induce an experimental PVR in rabbits that forms more rapidly and is more severe than that induced by ARPE-19 cells. To examine if knockdown of PI5P4K α and β could inhibit PVR in rabbits induced by RCFs, the expression of PI5P4K α and β was suppressed in RCFs by shRNA (Fig. 5A). Rabbit vitreous also induced an increase in PI5P4K α and β , as well as a decrease in p53 in these fibroblasts (Fig. 5A). Moreover, suppression of PI5P4K α and β reduced RCF contractability that was induced by RV (Fig. 5B). Therefore, we injected these cells and their

shGFP control cells intravitreally into rabbit eyes to compare their PVR potential. As shown in Figure 5C, shGFP RCFs led to development of severe PVR (stage 4 or 5). Typically in these stages, retinas get detached totally or close to this degree by day 7, whereas in this study, no rabbits that had been injected with shPI5P4K2A/B RCFs had developed any stage of PVR by day 7 (Fig. 5C). On day 28, the retinas of all rabbits injected with shGFP RCFs had completely detached retinas, while 60% of rabbits injected with shPI5P4K2A/B RCFs remained at stage 0 and 40% had progressed to stage 3 (Figs. 5C, 5D). These experiments indicate that inhibition of PI5P4K α and β can prevent severe PVR induced by intravitreal injection of RCFs in rabbits.

Knockdown of PI5P4K α and β in RPEM Cells Blocks HV-Induced Contraction

It is believed that RPE cells in ERMs contribute to the pathogenesis of PVR.⁹ Thus, we knocked down PI5P4K α and β in primary RPE cells isolated from an ERM of a PVR patient (RPEM) (Fig. 6A).³⁰ Intriguingly, HV also enhanced expression of PI5P4K α and β , and reduced p53 levels (Fig. 6A). These cells then were examined for their capability for HV-stimulated contraction in a collagen contraction assay. As shown in Figure 6B, suppression of PI5P4K α and β in RPEM cells blocked HV-induced contraction.

The above in vitro and in vivo observations indicate that vitreous-induced expression of PI5P4K α and β contributes to the pathogenesis of PVR. Thus, we wondered whether these two proteins were expressed in ERMs from PVR patients.⁷ As seen in Figure 6C, immunofluorescence staining revealed that both PI5P4K α and β were abundant in the tested ERMs from

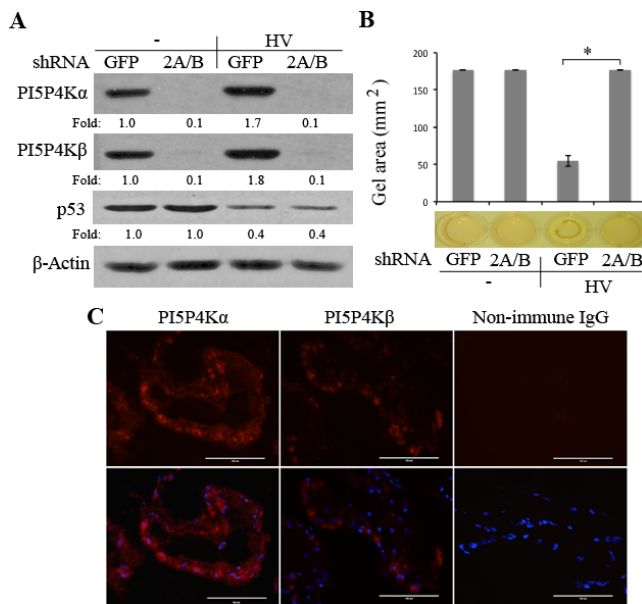


FIGURE 6. Suppression of PI5P4K α and β in RPEM cells inhibited HV-stimulated contraction. (A) Primary RPE cells from an epiretinal membrane of a PVR patient (RPEM) expressing shRNA for *GFP* (GFP) or *PIP4K2A/B* (2A/B) were treated for 16 hours with or without human PVR vitreous (HV) diluted (1:3) in DMEM/F12. The cell lysates were subjected to Western blot analysis using the antibodies indicated. This is representative of three independent experiments. (B) The characterized RPEM cells in (A) were examined for their ability to contract as described in the legend of Figure 2B. The mean \pm SD of the three independent experiments is shown; * $P < 0.05$ using an unpaired *t*-test. A photograph of a representative experiment is shown at the bottom of the bar graphs. (C) Frozen sections of epiretinal membranes from PVR patients were subjected to immunofluorescence analysis using antibodies against PI5P4K α and β or a normal rabbit IgG. Red signals indicate expression of PI5P4K α and β in comparison to the negative normal rabbit IgG stain control. This is representative of three independent experiments from epiretinal membranes of grade C PVR patients. Scale bar: 100 μ m.

grade C PVR patients and that they were localized to the membranes in virtually all the cells.

DISCUSSION

Phosphatidylinositol signaling has been shown to impact a variety of fundamental cellular processes, including intracellular membrane trafficking, cytoskeletal rearrangement, and cell proliferation, survival, and growth.⁴⁴ In this article, we demonstrate that vitreous stimulates a decrease in p53 and an increase in PI5P4K α and β , and that suppression of PI5P4K α and β impacted vitreous-induced cell proliferation, survival, migration, and contraction, as well as experimental PVR. It has been reported that depletion of PI5P4K α and β inhibits growth of p53-null tumors, where it was suggested that loss of both p53 and PI5P4K α and β leads to production of excess reactive oxygen species (ROS) that can lead to reduced cell proliferation and increased senescence.²⁶ Furthermore, the authors speculated that PI5P4K α and β are required to maintain glucose metabolism, thereby reducing oxidative phosphorylation and enhancing cell proliferation and survival when p53 is deficient.²⁶ We also speculated that a similar mechanism might be underlying the observed effects in PVR. Treatment of RPEs with vitreous leads to the activation of PDGFR/PI3K/Akt/MDM2, resulting in p53 reduction, and, concurrently, to the enhancement of PI5P4K α and β

expression and, in turn, to suppress the production of excess ROS, triggering cellular responses intrinsic to PVR.

In addition, PI5P4K α has been identified as essential for the clonogenic and leukemia-initiating potential of human acute leukemia cells, and it is required for these cells' proliferation and survival.⁴⁵ Knockdown of PI5P4K α in human acute leukemia cells results in accumulation of the cyclin-dependent kinase inhibitors (CDKNs) p21 and p27, G1 cell cycle arrest, and apoptosis.⁴⁵ However, knockdown of PI5P4K α in normal hematopoietic stem and progenitor cells does not adversely impact either clonogenic or multilineage differentiation potential.⁴⁵ Similarly, we found that suppression of both PI5P4K α and β did not affect RPE cell proliferation and contraction, but did influence vitreous-induced RPE cellular responses. These findings indicate a differential dependency and suggest that they might be a consequence of the regulation of different transcriptional programs in normal versus RV-induced conditions.

Both PI5P4K α and β are capable of phosphorylating PI-5-P on the fourth hydroxyl of the inositol ring to generate PI-4,5-P₂, which acts as a substrate for PI3K or phospholipase C to generate the essential second messengers PI-3,4,5-P₃ and IP₃, respectively.^{27,41,43,45,46} In addition, PI-4,5-P₂ can regulate actin filament elongation, interaction of the plasma membrane with the cytoskeleton, phagocytosis, clathrin-mediated endocytosis, and exocytosis.^{41,43,47-49} Vitreous-induced PI5P4K α and β that leads to increased migration and contraction in RPE cells may be mediated by these biochemical functions. However, it has been reported that knocking down PI5P4Ks activates the PI3K/Akt pathway in a subset of cancer cells, suggesting that the PI5P4Ks suppress PI3K/Akt signaling because they provide an alternative mechanism for enhancing glucose metabolism in response to ROS.²⁶

In this paper, we report that vitreous increased expression of both PI5P4K α and β . In addition, both PI5P4K α and β were abundant in ERMs from PVR patients. The fact that suppression of PI5P4K α and β inhibited only vitreous-induced cellular responses raises the possibility that inhibiting PI5P4K α and β might target only cells that have migrated into the vitreous. However, in this study, we used a cell injection rabbit model in which cell proliferation is not from endogenous cell proliferation. To better simulate PVR in clinics, a penetrating retinal injury rabbit model might be a way to test if a potential PI5P4K α inhibitor, such as tyrphostin AG-82,⁴⁴ would inhibit ocular trauma-induced PVR. Moreover, these experimental data might provide an option for the future therapeutic targeting of PI5P4K α and β to prevent PVR.

Acknowledgments

The authors thank Randy Huang for assistance in flow cytometry, Jessica Hoadley and Marie Ortega for their support with rabbit experiments, Oscar Morales for his assistance with OCT, Bianai Fan for histologic sections, and Gale Unger for copyediting this article.

Supported in full by National Institutes of Health (NIH) R01EY012509 (HL) and in part by NIH National Eye Institute Core Grant P30EY003790.

Disclosure: G. Ma, None; Y. Duan, None; X. Huang, None; C.X. Qian, None; Y. Chee, None; S. Mukai, None; J. Cui, None; A. Samad, None; J.A. Matsubara, None; A. Kazlauskas, None; P.A. D'Amore, None; S. Gu, None; H. Lei, None

References

- Morescalchi F, Duse S, Gambicorti E, Romano MR, Costagliola C, Semeraro F. Proliferative vitreoretinopathy after eye injuries: an overexpression of growth factors and cytokines leading to a retinal keloid. *Mediators Inflamm.* 2013;269787.

2. Abrams GW, Azen SP, McCuen BW II, Flynn HW Jr, Lai MY, Ryan SJ. Vitrectomy with silicone oil or long-acting gas in eyes with severe proliferative vitreoretinopathy: results of additional and long-term follow-up. Silicone Study Report 11. *Arch Ophthalmol*. 1997;115:335-344.
3. Pastor-Idoate S, Rodriguez-Hernandez I, Rojas J, et al. Genetics on PVRSG: the T309G MDM2 gene polymorphism is a novel risk factor for proliferative vitreoretinopathy. *PLoS One*. 2013; 8:e82283.
4. Casaroli-Marano RP, Pagan R, Vilaro S. Epithelial-mesenchymal transition in proliferative vitreoretinopathy: intermediate filament protein expression in retinal pigment epithelial cells. *Invest Ophthalmol Vis Sci*. 1999;40:2062-2072.
5. Connor TB Jr, Roberts AB, Sporn MB, et al. Correlation of fibrosis and transforming growth factor-beta type 2 levels in the eye. *J Clin Invest*. 1989;83:1661-1666.
6. Leaver PK, Billington BM. Vitrectomy and fluid/silicone-oil exchange for giant retinal tears: 5 years follow-up. *Graefes Arch Clin Exp Ophthalmol*. 1989;27:323-327.
7. Cui J, Lei H, Samad A, et al. PDGF receptors are activated in human epiretinal membranes. *Exp Eye Res*. 2009;88:438-444.
8. Schmidt GW, Broman AT, Hindman HB, Grant MP. Vision survival after open globe injury predicted by classification and regression tree analysis. *Ophthalmology*. 2008;115:202-209.
9. Agrawal RN, He S, Spee C, Cui JZ, Ryan SJ, Hinton DR. In vivo models of proliferative vitreoretinopathy. *Nat Protoc*. 2007;2: 67-77.
10. Cleary PE, Ryan SJ. Experimental posterior penetrating eye injury in the rabbit. II. Histology of wound, vitreous, and retina. *Br J Ophthalmol*. 1979;63:312-321.
11. Cleary PE, Ryan SJ. Experimental posterior penetrating eye injury in the rabbit. I. Method of production and natural history. *Br J Ophthalmol*. 1979;63:306-311.
12. Erdurman FC, Hurmeric V, Gokce G, Durukan AH, Sobaci G, Altinsoy HI. Ocular injuries from improvised explosive devices. *Eye (Lond)*. 2011;25:1491-1498.
13. Weichel ED, Colyer MH, Ludlow SE, Bower KS, Eiseman AS. Combat ocular trauma visual outcomes during operations Iraqi and Enduring Freedom. *Ophthalmology*. 2008;115:2235-2245.
14. Zhou Q, Xu G, Zhang X, Cao C, Zhou Z. Proteomics of post-traumatic proliferative vitreoretinopathy in rabbit retina reveals alterations to a variety of functional proteins. *Curr Eye Res*. 2012;37:318-326.
15. Vergara O, Ogden T, Ryan S. Posterior penetrating injury in the rabbit eye: effect of blood and ferrous ions. *Exp Eye Res*. 1989; 49:1115-1126.
16. Negrel AD, Thylefors B. The global impact of eye injuries. *Ophthalmic Epidemiol*. 1998;5:143-169.
17. Lei H, Velez G, Kazlauskas A. Pathological signaling via platelet-derived growth factor receptor α involves chronic activation of Akt and suppression of p53. *Mol Cell Biol*. 2011;31:1788-1799.
18. Haupt Y, Maya R, Kazaz A, Oren M. Mdm2 promotes the rapid degradation of p53. *Nature*. 1997;387:296-299.
19. Oliner JD, Kinzler KW, Meltzer PS, George DL, Vogelstein B. Amplification of a gene encoding a p53-associated protein in human sarcomas. *Nature*. 1992;358:80-83.
20. Vassilev LT, Vu BT, Graves B, et al. In vivo activation of the p53 pathway by small-molecule antagonists of MDM2. *Science*. 2004;303:844-848.
21. Lei H, Rheaume MA, Cui J, et al. A novel function of p53: a gatekeeper of retinal detachment. *Am J Pathol*. 2012;181:866-874.
22. Bond GL, Hu W, Bond EE, et al. A single nucleotide polymorphism in the MDM2 promoter attenuates the p53 tumor suppressor pathway and accelerates tumor formation in humans. *Cell*. 2004;119:591-602.
23. Dumont P, Leu JI, Della Pietra AC III, George DL, Murphy M. The codon 72 polymorphic variants of p53 have markedly different apoptotic potential. *Nat Genet*. 2003;33:357-365.
24. Pietsch EC, Humbey O, Murphy ME. Polymorphisms in the p53 pathway. *Oncogene*. 2006;25:1602-1611.
25. Pastor-Idoate S, Rodriguez-Hernandez I, Rojas J, et al. Genetics on PVRSG: the p53 codon 72 polymorphism (rs1042522) is associated with proliferative vitreoretinopathy: the Retina 4 Project. *Ophthalmology*. 2013;120:623-628.
26. Emerling BM, Hurov JB, Poulogiannis G, et al. Depletion of a putatively druggable class of phosphatidylinositol kinases inhibits growth of p53-null tumors. *Cell*. 2013;155:844-857.
27. Cantley LC. The phosphoinositide 3-kinase pathway. *Science*. 2002;296:1655-1657.
28. Sarkes D, Rameh LE. A novel HPLC-based approach makes possible the spatial characterization of cellular PtdIns5P and other phosphoinositides. *Biochem J*. 2010;428:375-384.
29. Walker DM, Urbe S, Dove SK, Tenza D, Raposo G, Clague MJ. Characterization of MTMR3, an inositol lipid 3-phosphatase with novel substrate specificity. *Curr Biol*. 2001;11:1600-1605.
30. Wong CA, Potter MJ, Cui JZ, et al. Induction of proliferative vitreoretinopathy by a unique line of human retinal pigment epithelial cells. *Can J Ophthalmol*. 2002;37:211-220.
31. Lei H, Velez G, Hovland P, Hirose T, Gilbertson D, Kazlauskas A. Growth factors outside the PDGF family drive experimental PVR. *Invest Ophthalmol Vis Sci*. 2009;50:3394-3403.
32. Lei H, Kazlauskas A. Growth factors outside of the PDGF family employ ROS/SFKs to activate PDGF receptor alpha and thereby promote proliferation and survival of cells. *J Biol Chem*. 2009;284:6329-6336.
33. Lei H, Velez G, Cui J, et al. N-Acetylcysteine suppresses retinal detachment in an experimental model of proliferative vitreoretinopathy. *Am J Pathol*. 2010;177:132-140.
34. Lei H, Qian CX, Lei J, Haddock LJ, Mukai S, Kazlauskas A. RasGAP promotes autophagy and thereby suppresses platelet-derived growth factor receptor-mediated signaling events, cellular responses, and pathology. *Mol Cell Biol*. 2015;35: 1673-1685.
35. Lei H, Rheaume MA, Velez G, Mukai S, Kazlauskas A. Expression of PDGFR α is a determinant of the PVR potential of ARPE19 cells. *Invest Ophthalmol Vis Sci*. 2011;52:5016-5021.
36. Andrews A, Balciunaite E, Leong FL, et al. Platelet-derived growth factor plays a key role in proliferative vitreoretinopathy. *Invest Ophthalmol Vis Sci*. 1999;40:2683-2689.
37. Fastenberg DM, Diddie KR, Sorgente N, Ryan SJ. A comparison of different cellular inocula in an experimental model of massive periretinal proliferation. *Am J Ophthalmol*. 1982;93: 559-564.
38. Giani A, Luiselli C, Esmaili DD, et al. Spectral-domain optical coherence tomography as an indicator of fluorescein angiography leakage from choroidal neovascularization. *Invest Ophthalmol Vis Sci*. 2011;52:5579-5586.
39. Giani A, Thanos A, Roh MI, et al. In vivo evaluation of laser-induced choroidal neovascularization using spectral-domain optical coherence tomography. *Invest Ophthalmol Vis Sci*. 2011;52:3880-3887.
40. Lei H, Romeo G, Kazlauskas A. Heat shock protein 90alpha-dependent translocation of annexin II to the surface of endothelial cells modulates plasmin activity in the diabetic rat aorta. *Circ Res*. 2004;94:902-909.
41. Carricaburu V, Lamia KA, Lo E, et al. The phosphatidylinositol (PI)-5-phosphate 4-kinase type II enzyme controls insulin

- signaling by regulating PI-3,4,5-trisphosphate degradation. *Proc Natl Acad Sci U S A*. 2003;100:9867–9872.
42. Bunney TD, Katan M. Phosphoinositide signalling in cancer: beyond PI3K and PTEN. *Nat Rev Cancer*. 2010;10:342–352.
 43. Jude JG, Spencer GJ, Huang X, et al. A targeted knockdown screen of genes coding for phosphoinositide modulators identifies PIP4K2A as required for acute myeloid leukemia cell proliferation and survival. *Oncogene*. 2015;34:1253–1262.
 44. Davis MI, Sasaki AT, Shen M, et al. A homogeneous, high-throughput assay for phosphatidylinositol 5-phosphate 4-kinase with a novel, rapid substrate preparation. *PLoS One*. 2013;8:e54127.
 45. Keune WJ, Jones DR, Bultsma Y, et al. Regulation of phosphatidylinositol-5-phosphate signaling by Pin1 determines sensitivity to oxidative stress. *Science Signal*. 2012;5:ra86.
 46. Keune WJ, Sims AH, Jones DR, et al. Low PIP4K2B expression in human breast tumors correlates with reduced patient survival: a role for PIP4K2B in the regulation of E-cadherin expression. *Cancer Res*. 2013;73:6913–6925.
 47. Mackey AM, Sarkes DA, Bettencourt I, Asara JM, Rameh LE. PIP4kgamma is a substrate for mTORC1 that maintains basal mTORC1 signaling during starvation. *Science Signal*. 2014;7:ra104.
 48. Haugsten EM, Oppelt A, Wesche J. Phosphatidylinositol 5-phosphate is a second messenger important for cell migration. *Commun Integr Biol*. 2013;6:e25446.
 49. Oppelt A, Haugsten EM, Zech T, et al. PIKfyve, MTMR3 and their product PtdIns5P regulate cancer cell migration and invasion through activation of Rac1. *Biochem J*. 2014;461:383–390.